*Computational Mechanics, 26(2000)*

# Meshless Local Petrov-Galerkin (MLPG) method in combination with finite element and boundary element approaches

G. R. Liu* and Y. T. Gu

Dept. of Mechanical and Production Engineering
National University of Singapore
10 Kent Ridge Crescent, Singapore 119260

## Abstract

The Meshless Local Petrov-Galerkin (MLPG) method is an effective truly meshless method for solving partial differential equations using Moving Least Squares (MLS) interpolants. It is, however, computationally expensive for some problems. A coupled MLPG/Finite Element (FE) method and a coupled MLPG/Boundary Element (BE) method are proposed in this paper to improve the solution efficiency. A procedure is developed for the coupled MLPG/FE method and the coupled MLPG/BE method so that the continuity and compatibility are preserved on the interface of the two domains where the MLPG and FE or BE methods are applied. The validity and efficiency of the MLPG/FE and MLPG/BE methods are demonstrated through a number of examples.

KEY WORDS: Meshless Method; Meshless Local-Galerkin Method; Finite element Method; Boundary Element Method; Stress Analysis

* Correspondence to: Gui-Rong LIU
Tel:+65-8746481 Fax: +65-7791459/8744795
E-mail: mpeliugr@nus.edu.sg, engp8973@nus.edu.sg

## 1. Introduction

Meshless methods have become recently attractive alternatives for problems in computational mechanics, as it does not require a mesh to discretize the problem domain, and the approximate solution is constructed entirely in terms of a set of scattered nodes. Some meshless methods are proposed and achieved remarkable progress, such as, Diffuse Element Method (DEM) (Nayroles et al. 1992), Element Free Galerkin (EFG) method (Belytschko et al. 1994), Reproducing Kernel Particle (RKP) method (Liu et al. 1995), Point Interpolation Method (PIM) (Liu and Gu 1999), Point Assembly Method (PAM) (Liu 1999), Boundary Node Method (BNM) (Mukherjee and Mukherjee 1997, Kothnur et al. 1999), Boundary Point Interpolation Method (BPIM) (Gu and Liu 1999a), and so on. In addition, techniques of coupling meshless methods with other established numerical methods have also been proposed, such as coupled EFG/Finite Element (FE) method (Belytschko and Organ 1995, Hegen 1996), EFG/Boundary Element (BE) method (Gu and Liu 1999b, Liu and Gu 2000a), and EFG/BPIM method (Liu and Gu 2000b).

In particular, the above-mentioned meshless methods are “meshless” only in terms of the interpolation of the field or boundary variables, as compared to the usual Finite Element Method(FEM) or Boundary Element Method (BEM). Most of meshless methods have to use background cells to integrate a weak form over the problem domain or boundary. The requirement of background cells for integration makes the method being not “truly” meshless.

Three truly meshless methods, called the Meshless Local Petrov-Galerkin (MLPG) method, the Local Boundary Integral Equation (LBIE) method, and the Local Point Interpolation Method (LPIM), have been developed by Atluri and Zhu (1998,2000a,b),

Atluri et al. (1999a,b), Zhu et al. (1998), Liu and Gu (2000b). The MLPG method is based on a local weak form and Moving Least Squares (MLS) approximation. In the MLPG, an integration method in a regular-shaped local domain (such as spheres, rectangular, and ellipsoids) is used. The MLPG method does not need any "element" or "mesh" for both field interpolation and background integration. The MLPG method has been used for two-dimensional elasto-statics (Atluri and Zhu 2000b) and one-dimensional 4th order thin beam static analysis (Atluri et al. 1999a). Very good results have been obtained.

However, there exist some inconvenience in using MLPG. First, it is difficult to implement essential boundary conditions in MLPG, because the shape functions, which constructed by MLS approximation, lack the delta function property. Second, the MLPG is computationally expensive due to again the use of MLS approximation. In addition, a local background integration cells structure has to be used for the integration, which can be computationally expensive for some problems, especially for problems with infinite or semi-infinite domains.

Some strategies have been developed to alleviate the above problems (Atluri et al. 1999b, Liu and Yan 2000). Alternatively, following the idea of the coupling of the EFG with FE and BE, these problems can also be overcome if the use of the MLPG method is limited to the sub-domain where their unique advantages are beneficial. In the remaining part of domain, FEM or BEM is employed.

It is often desirable and beneficial to combine two established numerical methods in order to exploit their advantages while evading their disadvantages. A lot of research work has been done in the coupled methods between two established numerical methods (Brebbia and Georgiou 1979, Rangogni and Reali 1982, Belytschko and Organ 1995,

Hegen 1996, Gu and Liu 1999b, Liu and Gu 2000a). Therefore, the idea of combining MLPG with other numerical techniques (FEM and BEM) is naturally of great interest in many practical applications.

This paper focuses on the coupling of the MLPG method with the FEM and BEM. Techniques for the coupled MLPG/FE method and the coupled MLPG/BE method for continuum mechanics problems are presented. The major difficulty of the coupling is to enforce the displacement compatibility conditions on the interface boundary between the MLPG domain and the FE domain or the BE domain. The interface elements, which are analogues to the FE interface element used by Gu and Liu (1999b), are formulated and used along the interface boundary. Within the interface element, the shape functions are comprised of the MLPG and FE shape functions. Shape functions constructed in this manner satisfy both consistency and compatibility conditions. However, the derivative of the modified interface shape function is discontinuous across the boundary between purely MLPG domain and the interface domain. It will make an additional difficulty in obtaining an accurate numerical integration. A technique is presented for numerical integration to divide the local integration domain into integration sub-cells by boundaries of FE interface elements.

Programs of coupled methods have been developed in FORTRAN, and a number of numerical examples are presented to demonstrate the convergence, validity and efficiency of the coupled methods.

## 2. MLPG formulation

### 2.1 Moving Least Squares interpolant

Consider a problem domain $\Omega$. To approximate a function $u(\mathbf{x})$ in $\Omega$, a finite set of $\mathbf{p}(\mathbf{x})$ called basis functions is considered in the space coordinates $\mathbf{x}^T=[x, y]$. The basis functions in two-dimension is given by

$$\mathbf{p}^T(\mathbf{x})=[1, x, y, x^2, xy, y^2\ldots] \tag{1}$$

The MLS interpolant $u^h(x)$ is defined in the domain $\Omega$ by

$$u^h(\mathbf{x}) = \sum_{j=1}^{m} p_j(\mathbf{x})a_j(\mathbf{x}) = \mathbf{p}^T(\mathbf{x})\mathbf{a}(\mathbf{x}) \tag{2}$$

where $m$ is the number of basis functions, the coefficient $a_j(x)$ in equation (2) is also functions of $\mathbf{x}$; $\mathbf{a}(\mathbf{x})$ is obtained at any point $\mathbf{x}$ by minimizing a weighted discrete $\mathbf{L}_2$ norm of:

$$J = \sum_{i=1}^{n} w(\mathbf{x}-\mathbf{x}_i)[\mathbf{p}^T(\mathbf{x}_i)\mathbf{a}(\mathbf{x}) - u_i]^2 \tag{3}$$

where $n$ is the number of points in the neighborhood of $\mathbf{x}$ for which the weight function $w(\mathbf{x}\text{-}\mathbf{x}_i)\neq 0$, and $u_i$ is the nodal value of $u$ at $\mathbf{x}=\mathbf{x}_i$ .

The stationarity of $J$ with respect to $\mathbf{a}(\mathbf{x})$ leads to the following linear relation between $\mathbf{a}(\mathbf{x})$ and $u_i$:

$$\mathbf{A}(\mathbf{x})\mathbf{a}(\mathbf{x})=\mathbf{B}(\mathbf{x})\mathbf{u} \tag{4}$$

Solving $\mathbf{a}(\mathbf{x})$ from equation (4) and substituting it into equation (2), we have

$$u^h(\mathbf{x}) = \sum_{i=1}^{n} \phi_i(\mathbf{x})u_i \tag{5}$$

where the MLS shape function $\phi_i(\mathbf{x})$ is defined by

$$\phi_i(\mathbf{x}) = \sum_{j=1}^{m} p_j(\mathbf{x})(\mathbf{A}^{-1}(\mathbf{x})\mathbf{B}(\mathbf{x}))_{ji} \tag{6}$$

where $\mathbf{A}(\mathbf{x})$ and $\mathbf{B}(\mathbf{x})$ are the matrices defined by

$$\mathbf{A}(\mathbf{x}) = \sum_{i=1}^{n} w_i(\mathbf{x})\mathbf{p}^{\mathrm{T}}(\mathbf{x}_i)\mathbf{p}(\mathbf{x}_i), \quad w_i(\mathbf{x})=w(\mathbf{x}-\mathbf{x}_i) \tag{7}$$

$$\mathbf{B}(\mathbf{x})=[w_1(\mathbf{x})\mathbf{p}(\mathbf{x}_1), w_2(\mathbf{x})\mathbf{p}(\mathbf{x}_2),\ldots,w_n(\mathbf{x})\mathbf{p}(\mathbf{x}_n)] \tag{8}$$

It can be found from above discussion that the MLS approximation does not pass through the nodal parameter values. Therefore the MLS shape functions given in equation (6) do not, in general, satisfy the Kronecker delta condition. Thus,

$$\phi_i(\mathbf{x}_j) \neq \delta_{ij} = \begin{cases} 1 & i = j \\ 0 & i \neq j \end{cases} \tag{9}$$

**2.2 Discrete equations of MLPG**

We consider the following two-dimensional problem of solid mechanics in domain $\Omega$ bounded by $\Gamma$ :

$$\nabla\boldsymbol{\sigma}+\mathbf{b}=0 \qquad \text{in } \Omega \tag{10}$$

where $\sigma$ is the stress tensor, which corresponds to the displacement field $\mathbf{u}=\{u, v\}^{\mathrm{T}}$, $\mathbf{b}$ is the body force vector, and $\nabla$ is the divergence operator. The boundary conditions are given as follows:

$$\sigma \cdot \mathbf{n} = \bar{\mathbf{t}} \qquad \text{on the natural boundary } \Gamma_t \tag{11}$$

$$\mathbf{u} = \bar{\mathbf{u}} \qquad \text{on the essential boundary } \Gamma_u \tag{12}$$

in which the superposed bar denotes the prescribed boundary values and $\mathbf{n}$ is the unit outward normal to domain $\Omega$.

Because the MLS shape functions lack the Kronecker delta function property, the accurate and efficient imposition of essential boundary condition often presents difficulties. Strategies have been developed to overcome this problem, such as Lagrange multipliers method (Belytschko et al. 1994), FE method (Krongauz and Belytschko

1995), penalty method (Zhu and Atluri 1998, Liu and Yang 1999) and direct interpolation method (Liu and Yan 2000). The essential boundaries of many problems can be included in the FE or BE domain purposely in the coupled methods. Therefore, the essential boundary conditions can be satisfied using the conventional manner in the FEM and BEM. For some problems, which the essential boundaries are difficult to be included in the FE domain or the BE domain, the method of enforcement of essential boundary conditions using interface finite elements can be adopted (Krongauz and Belytschko 1995).

A local weak form of the differential equation (10), over a local sub-domain $\Omega_s$ bounded by $\Gamma_s$, can be obtained using the weighted residual method

$$\int_{\Omega_s} w_i(\sigma_{ij,j} + b_i)\mathrm{d}\Omega = 0 \tag{13}$$

where $w_i$ is the weight function.

The first term on the left hand side of equation (13) can be integrated by parts to become

$$\int_{\Gamma_s} w_i \sigma_{ij} n_j \mathrm{d}\Gamma - \int_{\Omega_s} (w_{i,j}\sigma_{ij} - w_i b_i)\mathrm{d}\Omega = 0 \tag{14}$$

The support sub-domain $\Omega_s$ of a node $x_i$ is a domain in which $w_i(x)\neq 0$. A arbitrary shape support domain can be used. A circle or rectangular support domain is used in this paper for convenience. From Figure 1, it can be found that the boundary $\Gamma_s$ for the support domain is usually composed by three parts: the internal boundary $\Gamma_{si}$, the boundaries $\Gamma_{su}$ and $\Gamma_{st}$, over which the essential and natural boundary conditions are specified.

Imposing the natural boundary condition and noticing that $\sigma_{ij} n_j = \dfrac{\partial u}{\partial n} \equiv t_i$ in equation (14), we obtain:

$$\int_{\Gamma_{si}} w_i t_i \mathrm{d}\Gamma + \int_{\Gamma_{su}} w_i t_i \mathrm{d}\Gamma + \int_{\Gamma_{st}} w_i \bar{t}_i \mathrm{d}\Gamma - \int_{\Omega_s} (w_{i,j}\sigma_{ij} - w_i b_i)\mathrm{d}\Omega = 0 \tag{15}$$

For a support domain located entirely within the global domain, there is no intersection between $\Gamma_s$ and the global boundary $\Gamma$, $\Gamma_{si}=\Gamma_s$, and the integrals over $\Gamma_{su}$ and $\Gamma_{st}$ vanish.

With equation (15) for any node $x_i$, instead of dealing with a global boundary value problem, the problem becomes to deal with a localized boundary value problem over a support domain.

The problem domain $\Omega$ is represented by properly scattered nodes. The point interpolation approximation (5) is used to approximate the value of a point $x_Q$. Substituting equation (5) into the local weak form (15) for all nodes leads to the following discrete system equations

$$\mathbf{K}_{(\mathrm{MLPG})}\mathbf{u}_e = \mathbf{f}_{(\mathrm{MLPG})} \tag{16}$$

where the "stiffness" matrix $\mathbf{K}_{(\mathrm{MLPG})}$ and nodal "load" $\mathbf{f}_{(\mathrm{MLPG})}$ vector are defined by

$$\mathbf{K}_{(\mathrm{MLPG})ij} = \int_{\Omega_s} \mathbf{v}_i^{\mathrm{T}} \mathbf{D}\mathbf{B}_j \mathrm{d}\Omega - \int_{\Gamma_{si}} \mathbf{w}_i \mathbf{N}\mathbf{D}\mathbf{B}_j \mathrm{d}\Gamma - \int_{\Gamma_{su}} \mathbf{w}_i \mathbf{N}\mathbf{D}\mathbf{B}_j \mathrm{d}\Gamma \tag{17a}$$

$$\mathbf{f}_{(\mathrm{MLPG})i} = \int_{\Gamma_{st}} \mathbf{w}_i \bar{\mathbf{t}}_i \mathrm{d}\Gamma + \int_{\Omega_s} \mathbf{w}_i \mathbf{b}_i \mathrm{d}\Omega \tag{17b}$$

with $\mathbf{w}$ being the value of the weight function matrix, corresponding to node $i$, evaluated at the point $x$, and

$$\mathbf{N} = \begin{bmatrix} n_x & 0 & n_y \\ 0 & n_y & n_x \end{bmatrix} \tag{17c}$$

$$\mathbf{B}_j = \begin{bmatrix} \phi_{j,x} & 0 \\ 0 & \phi_{j,y} \\ \phi_{j,y} & \phi_{j,x} \end{bmatrix} \tag{17d}$$

$$\mathbf{v}_i = \begin{bmatrix} w_{i,x} & 0 \\ 0 & w_{i,y} \\ w_{i,y} & w_{i,x} \end{bmatrix} \tag{17e}$$

$$\mathbf{D} = \begin{bmatrix} 1 & \upsilon & 0 \\ \upsilon & 1 & 0 \\ 0 & 0 & (1-\upsilon)/2 \end{bmatrix} \quad \text{for plane stress} \tag{17f}$$

As the MLPG is regarded as a weighted residual method, the weight function plays an important role in the performance of the method. Theoretically, as long as the condition of continuity is satisfied, any weight function is acceptable. However, the local weak form is based on the local sub-domains centered by nodes. It can be found that the weight function with the local property, which should decrease in magnitude as the distance from a point $x_Q$ to the node $x_i$ increases, yields better results. Therefore, we will consider weight functions, which only depend on the distance between two points, such as the spline weight functions. It can be easily seen that the system stiffness matrix $\mathbf{K}_{(\mathrm{MLPG})}$ in the present method is banded but usually asymmetric. However, similarly as Galerkin FE methods, the weight function, $w$, can be take as the same formulation as equation (5). In this case $\mathbf{K}_{(\mathrm{MLPG})}$ becomes symmetrical (Atluri et al. 1999b). This symmetrical stiffness matrix can be an added advantage in applying the MLPG method.

## 3. FE formulation

The weak formulation of FEM for equation (10) is posed as follows

$$\int_{\Omega} \delta(\nabla_s \mathbf{u}^T) \cdot \sigma \mathrm{d}\Omega - \int_{\Omega} \delta\mathbf{u}^T \cdot \mathbf{b} \mathrm{d}\Omega - \int_{\Gamma_t} \delta\mathbf{u}^T \cdot \bar{\mathbf{t}} \mathrm{d}\Gamma = 0 \tag{18}$$

The interpolation form of FEM can be written as

$$u = \sum_{i=1}^{n_e} N_i(x) u_i \qquad n_e=3,4,5,\ldots.. \tag{19}$$

where $n_e$ is the number of nodes in a FE element, and the $N$ is the FE shape function.

Substituting the expression of $u$ and $v$ given in equation (19) into the weak form (18) yields

$$\mathbf{K}_{(\mathrm{FE})}\mathbf{u}_e = \mathbf{f}_{(\mathrm{FE})} \tag{20}$$

where

$$\mathbf{K}_{(\mathrm{FE})ij} = \int_{\Omega} \mathbf{B}_i^{\mathrm{T}} \mathbf{D} \mathbf{B}_j \mathrm{d}\Omega \tag{21a}$$

$$\mathbf{f}_{(\mathrm{FE})i} = \int_{\Gamma_t} N_i \bar{\mathbf{t}} \mathrm{d}\Gamma + \int_{\Omega} N_i \mathbf{b} \mathrm{d}\Omega \tag{21b}$$

$$\mathbf{B}_i = \begin{bmatrix} N_{i,x} & 0 \\ 0 & N_{i,y} \\ N_{i,y} & N_{i,x} \end{bmatrix} \tag{21c}$$

## 4. BE formulation

From equations (10)~(12), the principle of virtual displacements for linear elastic materials can be written as (Brabbia 1978):

$$\int_{\Omega} (\nabla\sigma + \mathbf{b}) \cdot \mathbf{u}^* \mathrm{d}\Omega = \int_{\Gamma_u} (\mathbf{u} - \bar{\mathbf{u}}) \cdot \mathbf{p}^* \mathrm{d}\Gamma - \int_{\Gamma_t} (\mathbf{p} - \bar{\mathbf{p}}) \mathbf{u}^* \mathrm{d}\Gamma \tag{22}$$

where $\mathbf{p}$ is the surface traction, $\mathbf{u}^*$ is the virtual displacement and $\mathbf{p}^*$ is the virtual surface traction corresponding to $\mathbf{u}^*$. The first term on the left-hand-side of equation

(22) is integrated by parts and used the fundamental solution (Brebbia et al 1984) to become

$$c_i u_i + \int_\Gamma \mathbf{up}^* d\Gamma = \int_\Gamma \mathbf{pu}^* d\Gamma + \int_\Omega \mathbf{bu}^* d\Omega \tag{23}$$

where $c$ is the constant depended on the shape of boundary. Consider the case that the boundary values of **u** and **p** are given by interpolation functions and the values at the nodes

$$\mathbf{u} = \mathbf{\Phi}^T \mathbf{u}_e \tag{24a}$$

$$\mathbf{p} = \mathbf{\Psi}^T \mathbf{p}_e \tag{24b}$$

where $\mathbf{\Phi}^T$ and $\mathbf{\Psi}^T$ are interpolation functions, $\mathbf{u}_e$ and $\mathbf{p}_e$ are the values of **u** and **p** of boundary nodes. The resulting boundary integral equation (23) can be written in matrix form as

$$\mathbf{H}\mathbf{u}_e = \mathbf{G}\mathbf{p}_e + \mathbf{d} \tag{25}$$

where

$$\mathbf{H} = \mathbf{c}_i + \int_\Gamma \mathbf{p}^* \mathbf{\Phi}^T d\Gamma \tag{26a}$$

$$\mathbf{G} = \int_\Gamma \mathbf{u}^* \mathbf{\Psi}^T d\Gamma \tag{26b}$$

$$\mathbf{d} = \int_\Omega \mathbf{u}^* \mathbf{b} d\Gamma \tag{26b}$$

In order to combine the BEM region with MLPG region together, the BE formulation is converted to equivalent MLPG formulation. Let us transform equation (25) by inverting **G** and multiply the result by the distribution matrix **M** (Brebbia et al 1984)

$$(\mathbf{M}\mathbf{G}^{-1}\mathbf{H})\mathbf{u}_e - (\mathbf{M}\mathbf{G}^{-1}\mathbf{d}) = \mathbf{M}\mathbf{p}_e \tag{27}$$

where distribution matrix **M** is defined as

$$\mathbf{M} = \int_\Gamma \Phi \Psi^T d\Gamma \tag{28}$$

we can now define:

$$\mathbf{K}_{(BE)}'=\mathbf{M}\mathbf{G}^{-1}\mathbf{H} \tag{29a}$$

$$\mathbf{f}_{(BE)}=\mathbf{M}\mathbf{p}_e+\mathbf{M}\mathbf{G}^{-1}\mathbf{d} \tag{29b}$$

Hence equation (34) has the following equivalent BEM form:

$$\mathbf{K}_{(BE)}'\,\mathbf{u}_e = \mathbf{f}_{(BE)} \tag{30}$$

The equivalent BE stiffness matrix $\mathbf{K}_{(BE)}'$ is generally asymmetric. The asymmetry arises from the approximations involved in the discretization process and the choice of the assumed solution. If the symmetric MLPG formulation is used, the symmetrization must be done for $\mathbf{K}_{(BE)}'$. One simple method is by minimizing the squares of the errors in the asymmetric off-diagonal terms of $\mathbf{K}_{(BE)}'$ (Brebbia et al 1984). Hence a new symmetric equivalent BE stiffness matrix $\mathbf{K}_{(BE)}$ can be obtained

$$K_{(BE)ij}=1/2(k_{(BE)ij}'+k_{(BE)ji}') \tag{31}$$

The equation (30) can be rewritten as:

$$\mathbf{K}_{(BE)}\,\mathbf{u}_e = \mathbf{f}_{(BE)} \tag{32}$$

# 5. Coupling of MLPG and FE or BE

## 5.1 Continuity conditions at coupled interfaces

Consider a problem domain consisting of two sub-domains $\Omega_1$ and $\Omega_2$, joined by an interface boundary $\Gamma_I$. The MLPG formulation is used in $\Omega_1$ and the FE or BE formulation is used in $\Omega_2$ as shown in Figure 1. Compatibility and equilibrium conditions on $\Gamma_I$ must be satisfied. Thus,

$$\mathbf{u}_I^{(1)}=\mathbf{u}_I^{(2)} \tag{33}$$

$$\mathbf{F}_I^{(1)}+\mathbf{F}_I^{(2)}=0 \tag{34}$$

where $\mathbf{u}_I^{(1)}$ and $\mathbf{u}_I^{(2)}$ are the displacement on $\Gamma_I$ for $\Omega_1$and $\Omega_2$, $\mathbf{F}_I^{(1)}$ and $\mathbf{F}_I^{(2)}$ are the forces on $\Gamma_I$ for $\Omega_1$and $\Omega_2$,respectively.

Because the shape functions of the MLPG method are derived using MLS, $\mathbf{u}^h$ in equation (5) differs with the nodal displacement value $\mathbf{u}$ at point $\mathbf{x}$. It is impossible to

couple MLPG and FE or BE domains directly along $\Gamma_I$. One simple method is to introduce interface elements in MLPG domain near the interface boundary $\Gamma_I$ (see Figure 1). In these interface elements, a hybrid displacement approximation is defined so that the shape functions of MLPG domain along $\Gamma_I$ possess the delta function property.

**5.2 Modified shape functions of interface elements**

The detailed characteristics of FE interface elements can be referred to Krongauz and Belytschko (1996). Because the nodal arrangement may be irregular in MLPG domain, 4~6 nodes isoparametric interface FE elements are used in this paper.

A detailed figure of interface domain is shown in Figure 1. $\Omega_I$ is a layer of sub-domain along the interface boundary $\Gamma_I$ within the MLPG domain $\Omega_1$. The new displacement approximation in MLPG domain $\Omega_1$ can be rewritten as:

$$\mathbf{u}_1^{\,h}(x) = \sum_i \tilde{\Phi}_i(x) u_i \tag{35}$$

where the hybrid shape functions of the interface element are defined as

$$\tilde{\Phi}_i(x) = \begin{cases} (1-R(x))\Phi_i(x) + R(x)N_i(x) & x \in \Omega_I \\ \Phi_i(x) & x \in \Omega_1 - \Omega_I \end{cases} \tag{36}$$

The derivatives of the interface shape functions are:

$$\tilde{\Phi}_{i,j} = \begin{cases} (1-R)\Phi_{i,j} - R_{,j}\Phi_i + RN_{i,j} + R_{,j}N_i & x \in \Omega_I \\ \Phi_{i,j} & x \in \Omega_1 - \Omega_I \end{cases} \tag{37}$$

Hence, the modified displacement approximation in domain $\Omega_1$ becomes

$$\mathbf{u}_1^{\,h}(\mathbf{x}) = \begin{cases} \mathbf{u}_{(\mathrm{MLPG})}(\mathbf{x}) + R(\mathbf{x})(\mathbf{u}_{(\mathrm{FE})}(\mathbf{x}) - \mathbf{u}_{(\mathrm{MLPG})}(\mathbf{x})) & \mathbf{x} \in \Omega_I \\ \mathbf{u}_{(\mathrm{MLPG})}(\mathbf{x}) & \mathbf{x} \in \Omega_1 - \Omega_I \end{cases} \tag{38}$$

where $\mathbf{u}_1^{\,h}$ is the displacement of a point in $\Omega_1$, $\mathbf{u}_{(\mathrm{MLPG})}$ is MLPG displacement given by equation(5), $\mathbf{u}_{(\mathrm{FE})}$ is FE displacement, the ramp function $R$ is equal to the sum of the FE

shape functions of a interface element associated with interface element nodes that are located on the interface boundary $\Gamma_{I,}$ i.e.

$$u_{(\mathrm{MLPG})}(\mathbf{x}) = \sum_{i=1}^{n} \phi_i(\mathbf{x}) u_i \tag{39a}$$

$$u_{(\mathrm{FE})} = \sum_{i=1}^{n_e} N_i(x) u_i \qquad n_e=3,4,5,\ldots.. \tag{39b}$$

$$R(x) \ = \sum_{i}^{k} N_i(x)\,, \quad x_i \in \Gamma_I \tag{39c}$$

where $\phi_i$ is the MLPG shape function given by equation(6), $N_i(x)$ is the FE shape function(see eg. Reddy 1993), $n_e$ is the number of nodes in an FE interface element, and $k$ is the number of nodes located on the interface boundary $\Gamma_I$ for a interface element. According the property of FE shape functions, $R$ will be unity along $\Gamma_I$ and vanish out of interface domain:

$$R(x) = \begin{cases} 1 & x \in \Gamma_I \\ 0 & x \in \Omega_1 - \Omega_I \end{cases} \tag{40}$$

The approximants (38) satisfy consistency and interpolate a linear field exactly, which is proved by Krongauz and Belytschko (1996). The regular MLPG and modified shape functions in 1-D are shown in Figure 2. In this figure, a two nodes linear interface element is used. It can be seen that the displacement approximation is continuous from purely MLPG domain ($\Omega_1$-$\Omega_I$) passing to the interface domain $\Omega_I$. The derivative of it is, however, discontinuous across the boundary. These discontinuities do not adversely affect the overall results since they only affect a small number of nodes (Krongauz and Belytschko 1996).

Using above approximants, the shape functions of MLPG domain along $\Gamma_I$ possess the Kronecker delta function property given in equation (9). The MLPG domain and FE or BE domain can be coupled directly.

### 5.3 Numerical integration in MLPG domain for coupled methods

A local numerical integration is needed to evaluate the integration in equation (17) in the MLPG domain. The Gauss quadrature is used. For a node $x_i$, a local regular-shaped integration cell (for example circle and rectangular) is needed to employ Gauss quadrature. For each Gauss quadrature point $x_Q$, the MLS interpolation is performed to obtain the integrand. Therefore, for a node $x_i$, there exist three local domains: local integration domain $\Omega_Q$ (same as $\Omega_s$, size $r_q$), weight function domain $\Omega_w$ for $w_i \neq 0$ (size $r_w$), and interpolation domain $\Omega_i$ for $x_Q$ (size $r_i$). These three local domains are independent as long as the condition $r_q \leq r_w$ is satisfied. It should be noted that if the weight function $w$ is taken zero along the boundary of integration domain, the equation (17b) can be simplified because the integration along the internal boundary $\Gamma_{si}$ vanishes.

There exit difficulties to obtain the exact numerical integration in meshless methods (Atluri et al. 1999b, Dolbow and Belytschko 1999). Insufficiently accurate numerical integration may cause a deterioration and a rank-deficiency in the numerical solution. The numerical integration errors are results from the complexities of the integrand. In order to guarantee the accuracy of the numerical integration, the $\Omega_Q$ should be divided into some regular small partitions. In each small partition, more Gauss quadrature points should be used.

Additional difficulty will be caused in the numerical integration when the local integration domain $\Omega_Q$ is inside or intersects with the interface domain $\Omega_I$. From the property of the interface shape function, it can be found that the derivative of the modified shape function is discontinuous across the boundary between purely MLPG

domain ($\Omega_1$-$\Omega_I$) and the interface domain $\Omega_I$. In addition, the derivative of the shape functions may be discontinuous across the boundary between two FE interface elements in term of the property of the FE shape function. The Gauss quadrature can fail to give the exact result for such discontinuous integrand regardless how many Gauss points are used. The difficulty can be overcome that the domain is divided into integration sub-domains by the boundaries of the interface elements (shown in the Figure 1 b). Then, the accurate integration can be obtained using Gauss quadrature.

## 6. Numerical result

Programs are developed to combine 3 ~6 nodes isoparametric FE(see eg. Reddy 1993) with MLPG, and constant, linear and quadratic BE with MLPG. Cases are run in order to examine the MLPG/FE and MLPG/BE in two-dimensional elastostatics. In the MLPG part, rectangle local domains are used for establishing weight function and obtaining numerical integration. The size of the local domain, $r_q$, for node $i$ and the size of the influence domain, $r_i$, for a point $x_Q$ are defined

$$r_q=\alpha d_e \tag{41a}$$

$$r_i=\beta d_e \tag{41b}$$

where, $\alpha$ and $\beta$ are coefficients chosen as 0.5~3.0 in this paper. The $d_e$ is the shortest distance between the node and neighbor nodes. Four nodes isoparametric FE interface elements are used in this paper.

### 6.1 Cantilever beam

Consider a beam of length $L$=48, height $D$=12, $E$=3.0×10$^7$, $\nu$=0.3, subjected to a parabolic traction at the free end with $P$=1000 as shown in Figure 3. The beam has a

unit thickness and a plane stress problem is considered. The analytical solution is available and can be found in a textbook by Timoshenko and Goodier (1970).

The beam is divided into two parts. BE and FE are used, respectively, in the part on the left part where the essential boundary is included. MLPG is used in the part on the right. The nodal arrangement is shown in Figure 4. Four nodes isoparametric rectangle finite elements are used in the FE part, and linear boundary elements are used in the BE part. Sixty three nodes are used in the MLPG part. The results for $\alpha$=1.5 and $\beta$=3.0 are obtained.

The function of interface element is investigated. In the absence of the interface elements, i.e. MLPG region are combined with FE or BE region directly along the interface boundary $\Gamma_I$, the vertical displacement results of right end of the beam are listed in the Table 1. It can be found that the absence of interface elements causes errors. It is apparent that interface elements are imperative in the combination MLPG with FE or BE.

It is found that for displacement, results obtained are identical. As the stress is most critical, detail results of shear stress are presented here. Figure 5 illustrates the comparison between the shear stress calculated analytically and by the coupled methods at the section of $x=L/2$. The plot shows an excellent agreement between the analytical and numerical results.

For quantitative error analysis, we define the following norm using shear stresses as an error indicator, as the accuracy in shear strain or shear stress is much more critical for the beam problem.

$$e_t = \frac{1}{N}\sqrt{\sum_{i=1}^{N}(\tau_i - \bar{\tau}_i)^2 \Big/ \sum_{i=1}^{N}\bar{\tau}^2} \tag{42}$$

where $N$ is the number of nodes investigated, $\tau$ is the shear stress obtained by numerical method, and $\bar{\tau}$ is the analytical shear stress.

The convergences for the coupled MLPG/FE method and the coupled MLPG/BE method with mesh refinement are shown in Figure 6, where $h$ is equivalent to the maximum element size in the finite element method in this case. It is observed that the convergences of the coupled methods are very good. The convergence of using the MLPG for whole domain is also shown in the same figure. It can be observed from this figure that the accuracy of the MLPG is the best in these three methods. The accuracy of MLPG/BE is higher than that of MLPG/FE because of the higher accuracy of BE than FE in obtaining stresses. However, the convergence rate of these two coupled methods is nearly same.

**6.2 Hole in an infinite plate**

A plate with a circular hole subjected to a unidirectional tensile load of 1.0 in the $x$ direction is considered. Due to symmetry, only the upper right quadrant (size 5×5) of the plate is modeled as shown in Figure 7. When the condition $b/a \geq 5$ is satisfied, the solution of finite plate is very closed to that of the infinite plate (Roark and Young, 1975). Plane strain condition is assumed, and $E=1.0\times10^3$, $\nu=0.3$. Symmetry conditions are imposed on the left and bottom edges, and the inner boundary of the hole is traction free. The tensile load in the $x$ direction is imposed on the right edge. The exact solution for the stresses of infinite plate is available and can be found in a textbook by Timoshenko and Goodier (1970).

The plate is divided into two parts, where MLPG is used in one part, FE and BE are applied in the other part, respectively. The nodal arrangements of coupled methods are shown in Figure 7. $\alpha$=1.0 and $\beta$=2.0 are used in the MLPG part. Four nodes finite elements and linear boundary elements are used, respectively, in the FE or BE part.

As the stress is most critical, detailed results on stress are presented here. The stress $\sigma_x$ at $x$=0 obtained by the coupled methods are plotted in Figure 8. The result obtained by MLPG is shown in the same figure. It can be observed from Figure 8 that the coupled methods yield satisfactory results for the problem considered.

### 6.3 Internal pressurized hollow cylinder

A hollow cylinder under internal pressure is shown in Figure 9. The parameters are taken as $p$=100, $G$=8000, and $\nu$=0.25. The analytical solution for this problem is available. Due to the symmetry of the problem, only one quarter of the cylinder needs to be modeled. The cylinder is divided into two parts, where MLPG and FE (4 nodes elements) or BE (linear elements) are applied, respectively. As shown in Figure 10, 96 nodes and 78 nodes are used to discretize the domain and boundary in MLPG/FE and MLPG/BE. The result of $\alpha$=1.0 and $\beta$=2.0 are obtained.

The MLPG/FE and MLPG/BE results are compared to the MLPG, and analytical solution. The radial displacements of boundary nodes are presented in Table 2. It can be found that The MLPG/FE and MLPG/BE results are in very good agreement with the analytical solution.

### 6.4 A structure on a semi-infinite foundation

In this example the coupled methods are used in an semi-infinite problem, which has been solved using coupled FE/BE method (Brebbia and Georgiou 1979) and the

coupled EFG/BE method (Gu and Liu 1999a). A structure stands on a semi-infinite foundation is shown in Figure 11. Loads are imposed on the structure. The infinite foundation can be treated in practice in either of the following three ways: by truncating the semi-infinite plane at a finite distance (approximate method), using a fundamental solution appropriate to the semi-space problem rather than a free-space Green's function in BEM, and using infinite element in FEM. The first approximate method is used because it is convenient to compare the coupled method solutions with the FE and FE/BE solutions.

As shown in Figure 11, Region 2 represents the semi-infinite foundation and is given a semi-circular shape of very large diameter in relation to Region 1 that represents the structure. Boundary conditions to restrain rigid body movements are applied. The MLPG is used in Region 1, and the FE and BE are used, respectively, in Region 2. The nodal arrangements of the coupled MLPG/BE method and the coupled MLPG/FE method are shown in Figures 11 and 12. The problem is also analyzed using FEM, MLPG and FE/BE methods. Two loading cases shown in Figure 13 are analyzed: Case 1 considers five concentrated vertical loads along the top and case 2 considers an additional horizontal load acting at the right corner.

The displacement results of top of the structure are given in Table 3. The results obtained using FEM, MLPG and FE/BE methods are included in the same table. The results obtained using the present MLPG/FE and MLPG/BE methods are in very good agreement with those obtained using FE, MLPG and FE/BE methods. However, it is interesting to note that the foundation is adequately represented using only 30 BE nodes in the coupling MLPG/BE case as compared to 120 for the MLPG cases. The saving is considerable.

## 7 Discussion and conclusions

The coupled MLPG/FE and MLPG/BE methods have been considered in this paper. In these coupled methods, the problem domain is divided into two (or several) parts. The MLPG is used in one part where MLPG method needed, and the FE or BE is used in other parts. Because the MLPG shape functions constructed using MLS approximation, the shape functions of MLPG along the combination boundary lack the Kronecker delta function property. In order to overcome this difficulty, the interface elements are defined with shape functions composed of the FE and MLPG shape functions along the combination boundary. The shape functions are constructed so that linear consistency is met exactly. Numerical examples have demonstrated the effectiveness of the present coupled MLPG/FE and MLPG/BE methods for 2-D elastostatics.

The present coupled methods can give full play of the advantages of both MLPG, FE and BE methods. First, the computation cost is much lower because the MLS approximation is only used in one part. Second, imposition of essential boundary conditions becomes easier in coupled methods than in the MLPG method. Third, the coupled methods are of great interest in many practical problems, such as using MLPG/BE to solve fluid-structure interaction problems with infinite or semi-infinite domains, and so on.

With above mentioned advantages, the coupled MLPG/FE and MLPG/BE methods offers a potential numerical alternative simple and efficient procedure for handling problems of industrial applications.

## Reference

**Atluri SN**, **Cho JY**, **Kim HG**(1999a) Analysis of thin beams, using the meshless local Petrov-Galerkin (MLPG) method, with generalized moving least squares interpolation.Computational Mechanics 24: 334-347

**Atluri SN**, **Kim HG, Cho JY**(1999b) A critical assessment of the truly meshless local Petrov-Galerkin (MLPG), and Local Boundary Integral Equation (LBIE) methods. Computational Mechanics 24:348-372

**Atluri SN, Zhu T** (1998) A new meshless local Petrov-Galerkin (MLPG) approach in computational mechanics. Computational Mechanics 22:117-127.

**Atluri SN, Zhu T**(2000a) New concepts in meshless methods. Int. J. Numer. Methods Engrg. 47 (2000) 537-556.

**Atluri SN, Zhu T** (2000b) The meshless local Petrov-Galerkin (MLPG) approach for solving problems in elsto-statics. Computational Mechanics 225:169-179

**Belytschko T**, **Lu YY**, **Gu L** (1994) Element-Free Galerkin methods. Int. J. Numer. Methods Engrg. 37:229-256

**Belytschko T**, **Organ D** (1995) Coupled finite element-element–free Galerkin method. Computational Mechanics 17:186-195

**Brebbia CA** (1978) The Boundary Element Method for Engineers. Pentech Press, London, Halstead Press, New York

**Brebbia CA, Georgiou P** (1979) Combination of boundary and finite elements in elastostics. Appl. Math. Modeling: 3 212-219

**Brebbia CA**, **Telles JC**, **Wrobel LC** (1984) Boundary Element Techniques. Springer Verlag, Berlin

**Dolbow J, Belytschko T** (1999) Numerical itegration of the Galerkin weak form in meshfree methods. Computational Mechanics 23: 219-230

**Gu Y T ,Liu GR** (1999a) A boundary point interpolation method for stress analysis of solids. submitted.

**Gu YT**, **Liu GR** (1999b) A coupled Element Free Galerkin/Boundary Element method for stress analysis of two-dimension solid. Computer Methods in Applied Mechanics and Engineering (in press)

**Hegen D** (1996) Element-free Galerkin methods in combination with finite element approaches. Comput. Methods Appl. Mech. Engrg. 135:143-166

**Krongauz Y., Belytschko T.**(1996) Enforcement of essential boundary conditions in meshless approximations using finite element. Comput. Methods in Appl. Mech. and Engrg.: 131 133-145

**Kothnur VS**, **Mukherjee S**, **Mukherjee YX**(1999) Two-dimensional linear elasticity by the boundary node method. Int. J. of Solids and Structures 36:1129-1147

**Liu GR** (1999) A Point Assembly Method for Stress Analysis for Solid. In: Shim VPW(ed) Impact Response of Materials & Structures. Oxford, pp 475-480

**Liu GR**, **Gu YT** (1999) A Point Interpolation Method for two-dimensional solid. Int. Journal for Numerical Methods in Eng. (in press)

**Liu GR**, **Gu YT**(2000a) Coupling Element Free Galerkin and Hybrid Boundary Element methods using modified variational formulation. Australasian Issue of Computational Mechanics 26: 166-173

**Liu GR**, **Gu YT** (2000b) Coupling of Element Free Galerkin method with Boundary Point Interpolation Method. ICES'2K,( Los Angles, 2000)

**Liu GR** , **Gu YT** (2000c) A Local Point Interpolation Method for stress analysis of two-dimensional solids. Int. J. Structural Engineering and Mechanics (accepted)

**Liu GR**, **Yang KY** (1998) A penalty method for enforce essential boundary conditions in element free Galerkin method. The proceeding of the 3rd HPC Asia'98. Singapore, pp 715-721

**Liu GR**, **Yan L** (2000) A Modified Meshless Local Petrov-Galerkin Method for Solid Mechanics. Submitted

**Liu WK**, **Jun S, Zhang YF**(1995) Reproducing kernel particle methods. Int. J. Numer. Methods Engrg. 20: 1081-1106

**Mukherjee YX, Mukherjee S** (1997) Boundary node method for potential problems. Int. J. Num. Methods in Engrg. 40: 797-815

**Nayroles B, Touzot G, Villon P** (1992) Generalizing the finite element method: diffuse approximation and diffuse elements. Comput. Mech. 10: 307-318

**Rangogni R, Reali M**. (1982) The coupling of the finite difference method and the boundary element method. Appl. Math. Modelling: 6 233-236

**Reddy JN** (1993) An introduction to the Finite Element Method. Second Edition, (McGraw-hill, New York, 1993).

**Roark RJ**., **Young WC**(1975) Formulas for stress and strain. McGrawhill, London

**Timoshenko SP**, **Goodier JN** (1970) Theory of Elasticity. 3rd Edition. McGraw-hill, New York

**Zhu T, Atluri SN** (1998) A modified collocation & a penalty formulation for enforcing the essential boundary conditions in the element free Galerkin method. Comput. Mech.:21:211-222

**Zhu T, Zhang JD, Atluri SN** (1998) A local boundary integral equation (LBIE) method in computational mechanics, and a meshless discretization approach. Computational Mechanics 21:223-235

**Table 1 Vertical displacement of the right end of the beam($\times 10^{-2}$)**

| | Analytical solution $u_y$ | MLPG/FE | | MLPG/BE | |
|---|---|---|---|---|---|
| | | $u_y$ | Error(%) | $u_y$ | Error(%) |
| **With interface elements** | 0.89 | 0.8605 | -2.81 | 0.8712 | -2.11 |
| **Without interface elements** | 0.89 | 0.7285 | -18.15 | 0.7232 | -18.74 |

**Table 2 Radial displacement for hollow cylinder($\times 10^{-2}$)**

| Nodes | Exact. | MLPG/FE | MLPG/BE | MLPG |
|---|---|---|---|---|
| 1 | 0.4464 | 0.4461 | 0.4468 | 0.4463 |
| 2 | 0.4464 | 0.4462 | 0.4473 | 0.4466 |
| 3 | 0.4464 | 0.4478 | 0.4488 | 0.4470 |
| 4 | 0.8036 | 0.8021 | 0.8120 | 0.8026 |
| 5 | 0.8036 | 0.8062 | 0.8116 | 0.8068 |
| 6 | 0.8036 | 0.8101 | 0.8112 | 0.8091 |

Liu and Gu : Tables 1&2

**Table 3 Vertical displacements along top of structure**

| Displacements ($\times 10^{-4}$) | | | | | |
|---|---|---|---|---|---|
| Load case 1 | | | | | |
| **Nodes** | **FE** | **MLPG** | **FE/BE** | **MLPG/FE** | **MLPG/BE** |
| 1 | 1.41 | 1.43 | 1.40 | 1.42 | 1.43 |
| 2 | 1.34 | 1.34 | 1.33 | 1.34 | 1.35 |
| 3 | 1.32 | 1.32 | 1.32 | 1.32 | 1.32 |
| 4 | 1.34 | 1.34 | 1.33 | 1.34 | 1.35 |
| 5 | 1.41 | .143 | 1.40 | 1.42 | 1.43 |
| Load case 2 | | | | | |
| 1 | -3.39 | -3.58 | -3.55 | -3.53 | -3.62 |
| 2 | -0.97 | -1.12 | -1.05 | -1.00 | -1.07 |
| 3 | 1.35 | 1.36 | 1.35 | 1.35 | 1.34 |
| 4 | 3.61 | 3.72 | 3.70 | 3.59 | 3.69 |
| 5 | 6.00 | 6.15 | 6.17 | 6.14 | 6.14 |

Liu and Gu : Table 3

## Tables and Figures Captions:

Table 1 Vertical displacement of the right end of the beam($\times 10^{-2}$)

Table 2 Radial displacement for hollow cylinder($\times 10^{-2}$)

Table 3 Vertical displacements along top of structure

Figure 1 Domain division into MLPG and FE or BE regions

(a)The interface elements; the weight function domain $\Omega_w$ and integration domain $\Omega_Q$ for node $i$; the interpolation domain $\Omega_i$ for Gauss integration point $x_Q$

(b) Detailed integration sub-domain $\Omega'_Q$ of $\Omega_Q$ for node $i$

Figure 2 Comparison of original and modified shape functions of MLPG region in 1-D

Figure 3 Cantilever beam

Figure 4 Nodal arrangement of the cantilever beam

Figure 5 Shear stress $\tau_{xy}$ at the section $x=L/2$ of the beam

Figure 6 Convergence in $e_t$ norm of error

Figure 7 Nodes in a plate with a central hole subjected to a unidirectional tensile load in the $x$ direction (a) MLPG/FE (b)MLPG/BE

Figure 8 Stress distribution obtained using MLPG/FE and MLPG/BE methods ($\sigma_x$, at $x=0$)

Figure 9 Hollow cylinder subjected to internal pressure

Figure 10 Arrangement of nodes for the hollow cylinder (a) MLPG/FE (b)MLPG/BE

Figure 11 Nodal arrangement of the coupled MLPG/BE method for the problem of a structure standing on a semi-infinite foundation

Figure 12 Nodal arrangement of the coupled MLPG/FE method

Figure 13 MLPG/FE detailed nodal arrangement of the structure and load cases

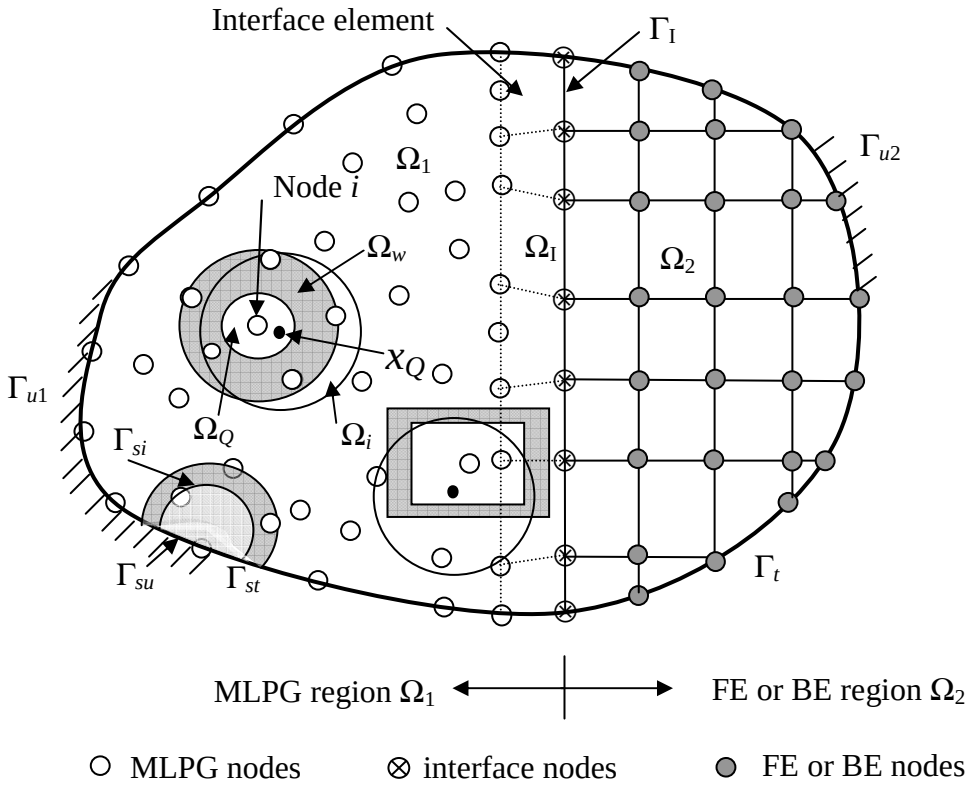


(a) The interface elements; the weight function domain $\Omega_w$ and integration domain $\Omega_Q$ for node $i$; the interpolation domain $\Omega_i$ for Gauss integration point $x_Q$

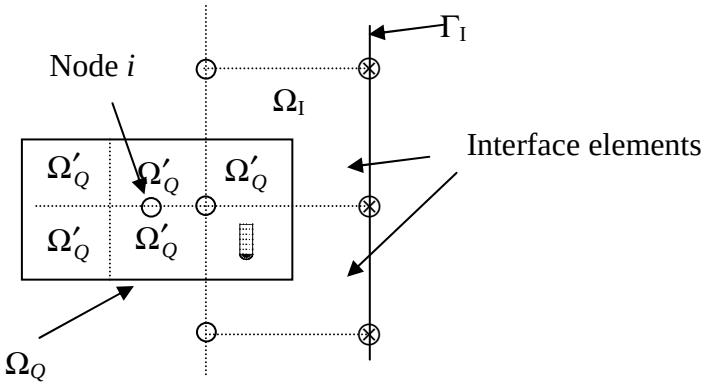


(b) Detailed integration sub-domain $\Omega'_Q$ of $\Omega_Q$ for node $i$

Figure 1 Domain division into MLPG and FE or BE regions

Liu and Gu : Figure 1

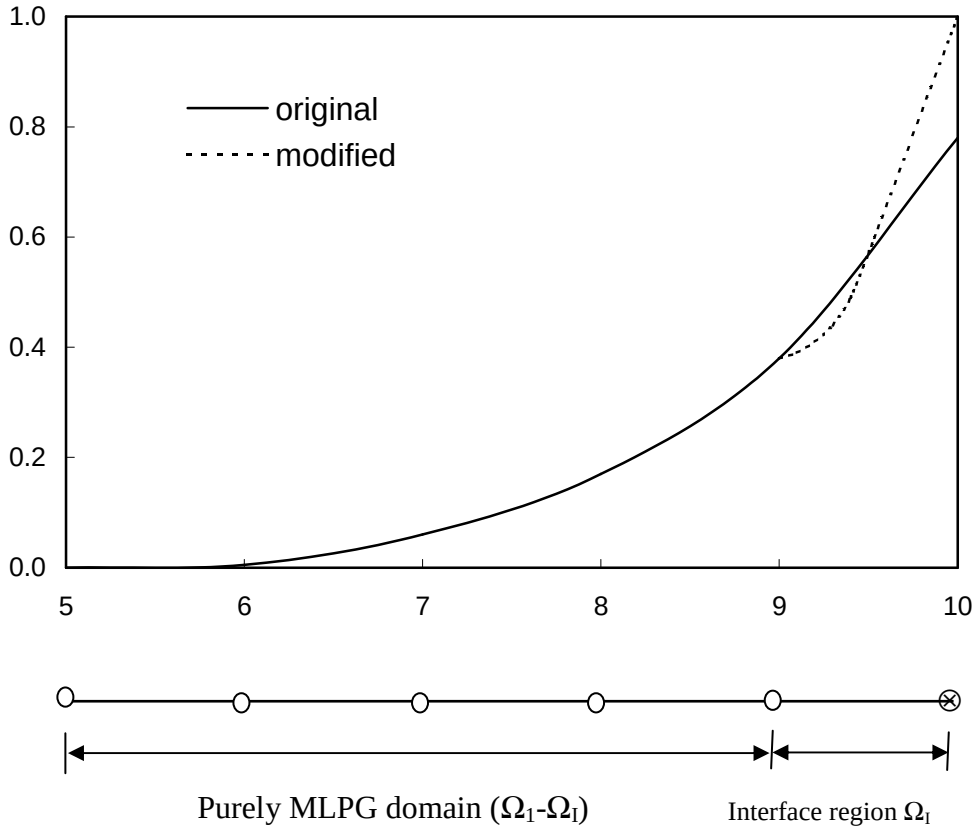


Figure 2 Comparison of original and modified shape functions of MLPG region in 1-D

Liu and Gu : Figure 2

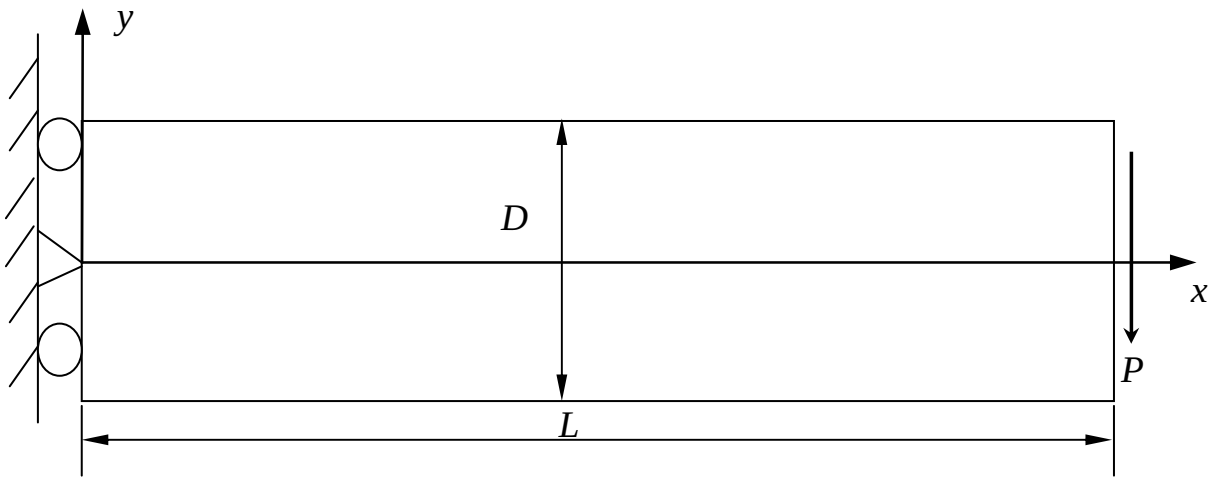


Figure 3 Cantilever beam

Liu and Gu : Figure 3

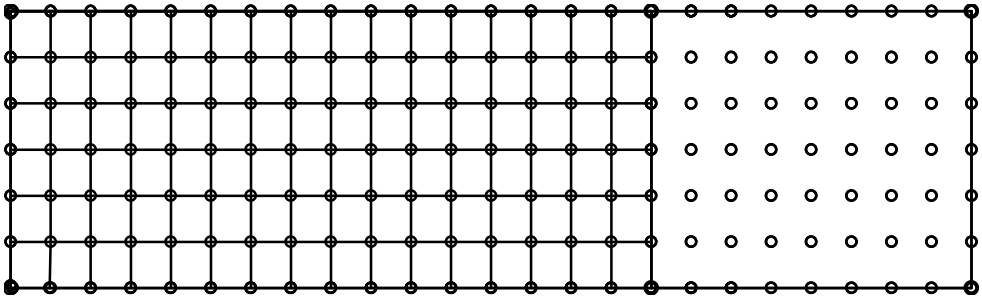

(a)

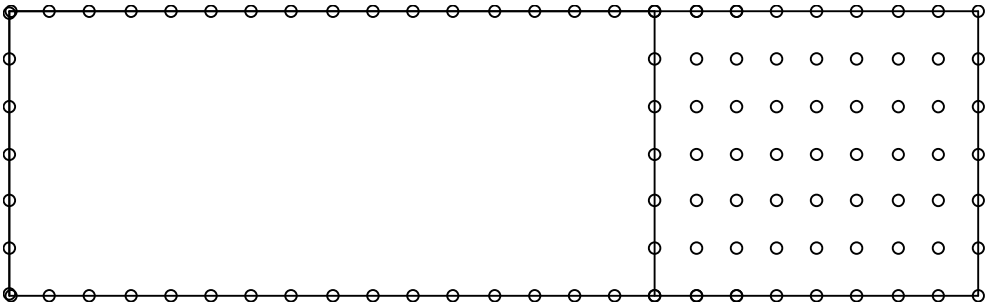

(b)

Figure 4 Nodal arrangement of the cantilever beam

Liu and Gu : Figure 4

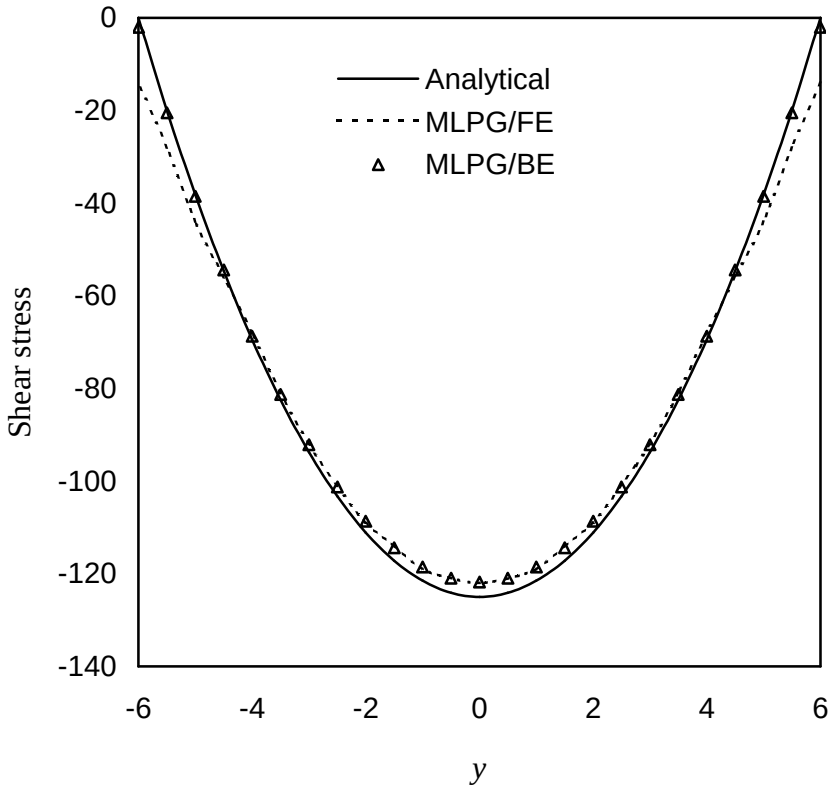


Figure 5 Shear stress $\tau_{xy}$ at the section $x=L/2$ of the beam

Liu and Gu : Figure 5

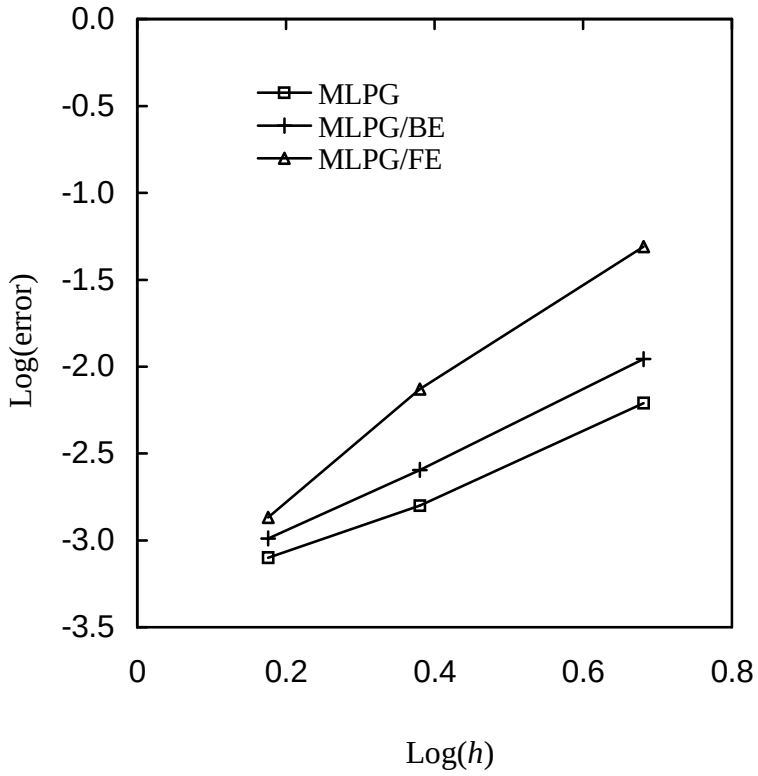


Figure 6 Convergence in $e_t$ norm of error

Liu and Gu : Figure 6

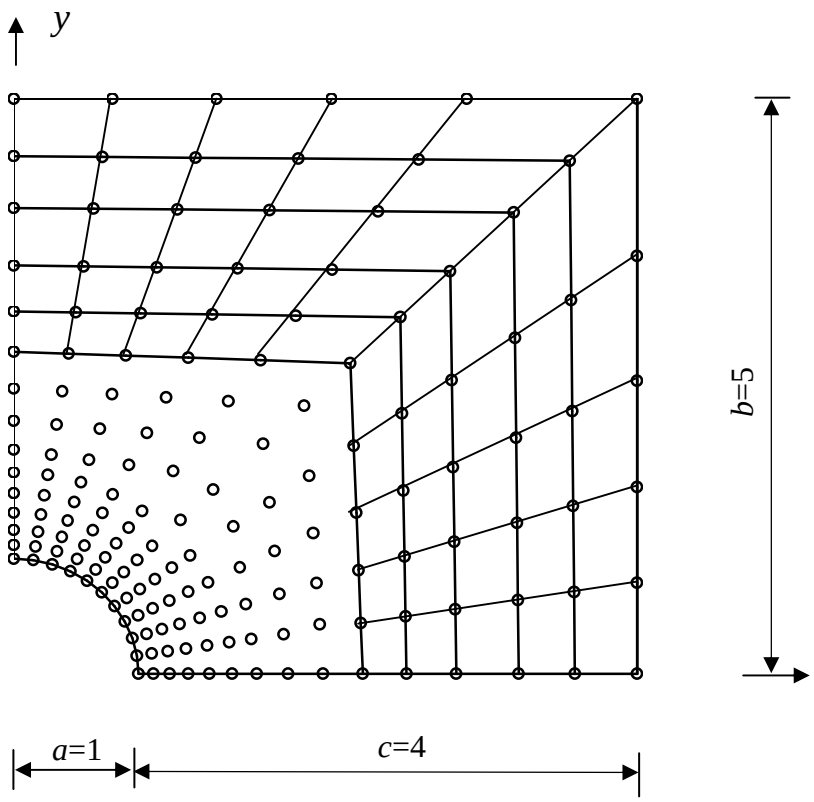


(a) MLPG/FE

Liu and Gu : Figure 7(a)

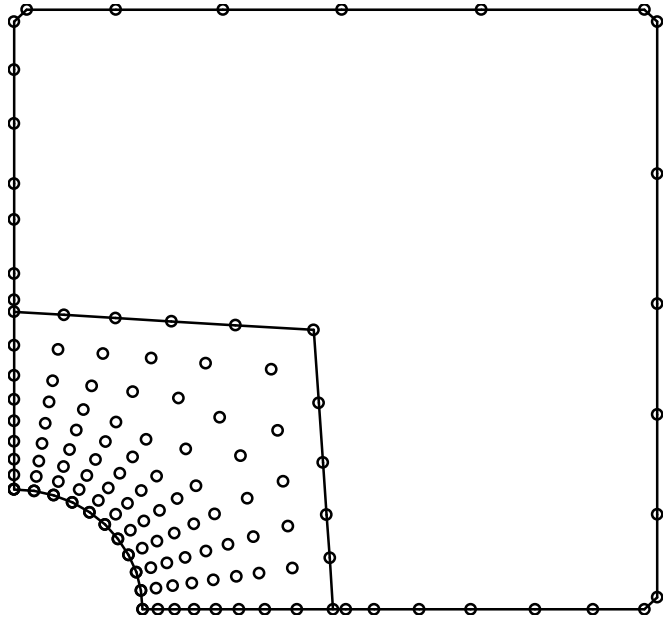

(b) MLPG/BE

Figure 7 Nodes in a plate with a central hole subjected to a unidirectional tensile load in the *x* direction

Liu and Gu : Figure 7(b)

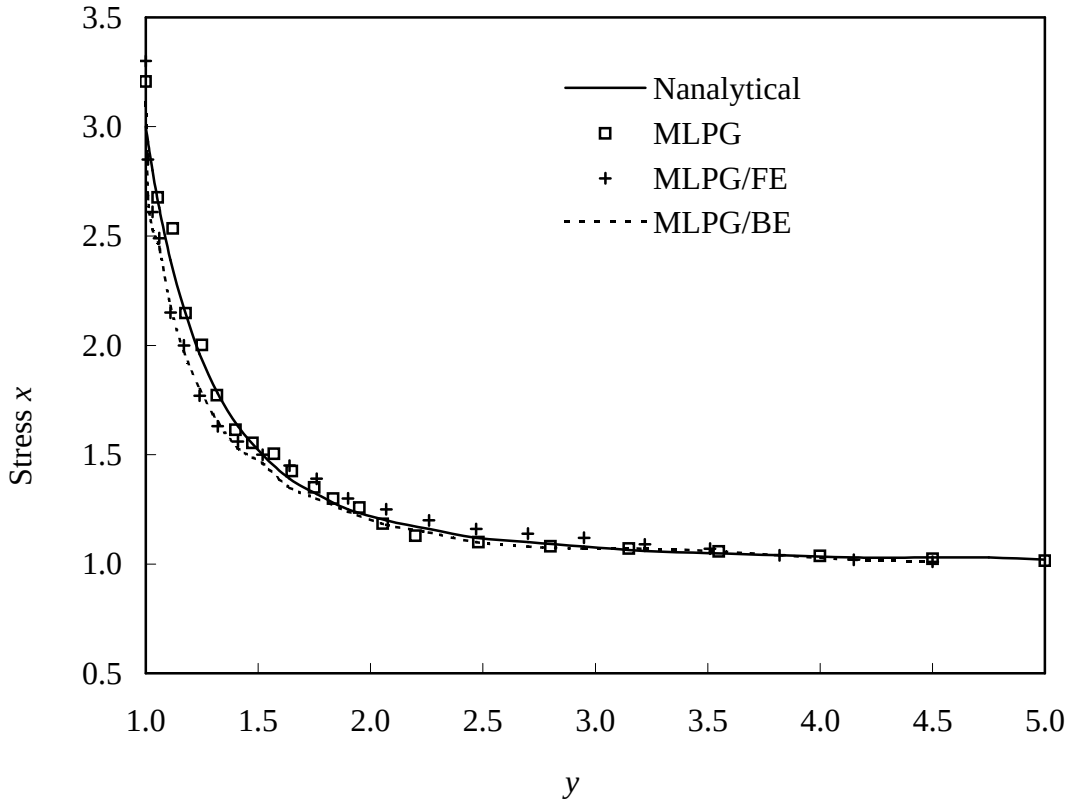


Figure 8 Stress distribution obtained using MLPG/FE and MLPG/BE methods ($\sigma_x$, at $x$=0)

Liu and Gu : Figure 8

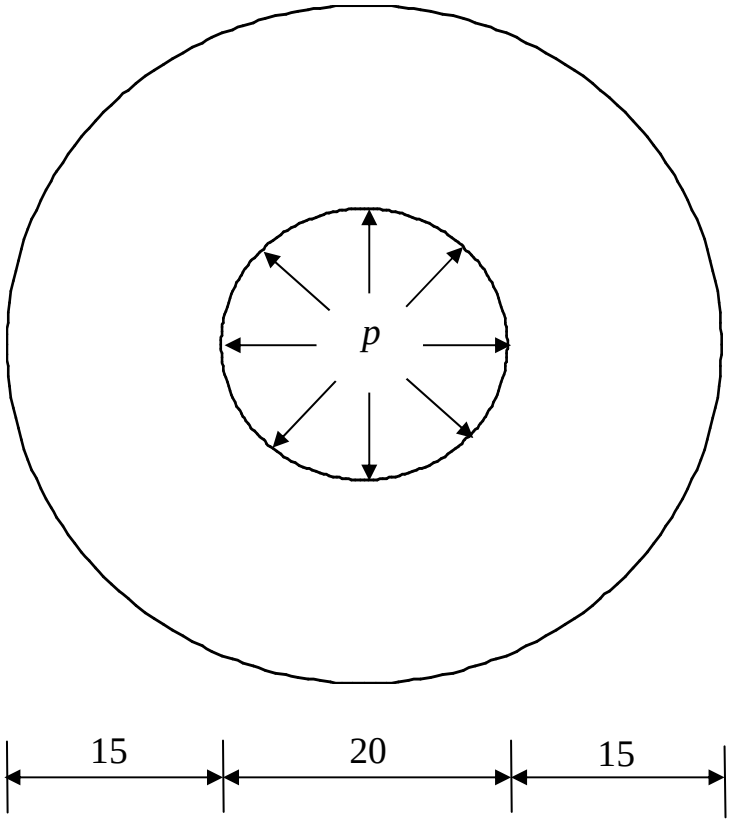


Figure 9 Hollow cylinder subjected to internal pressure

Liu and Gu : Figure 9

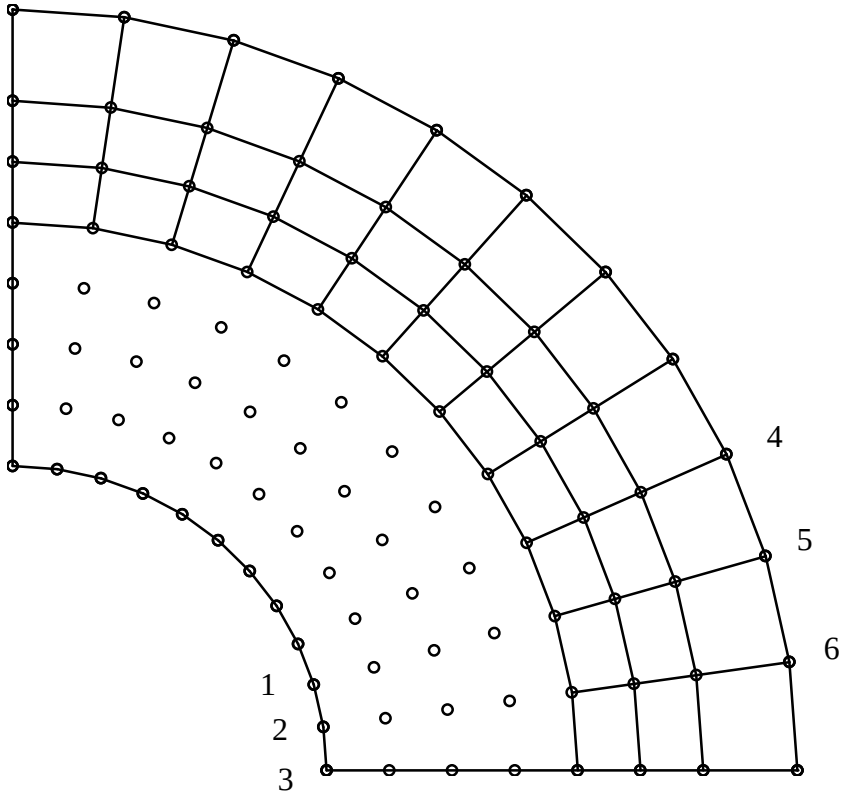


(a) MLPG/FE

Liu and Gu : Figure 10(a)

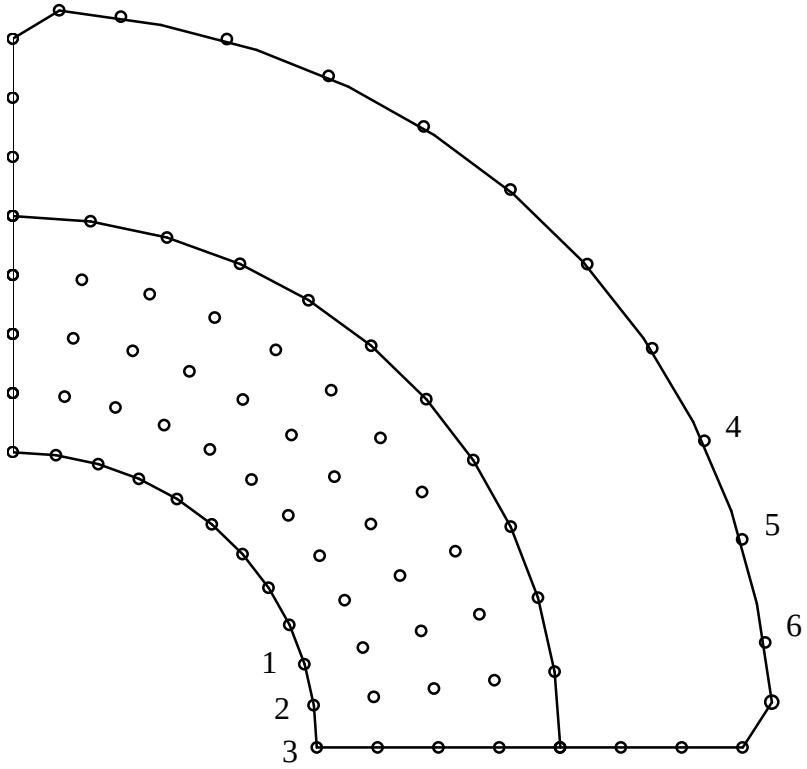


(b) MLPG/BE

Figure 10 Arrangement of nodes for the hollow cylinder

Liu and Gu : Figure 10(b)

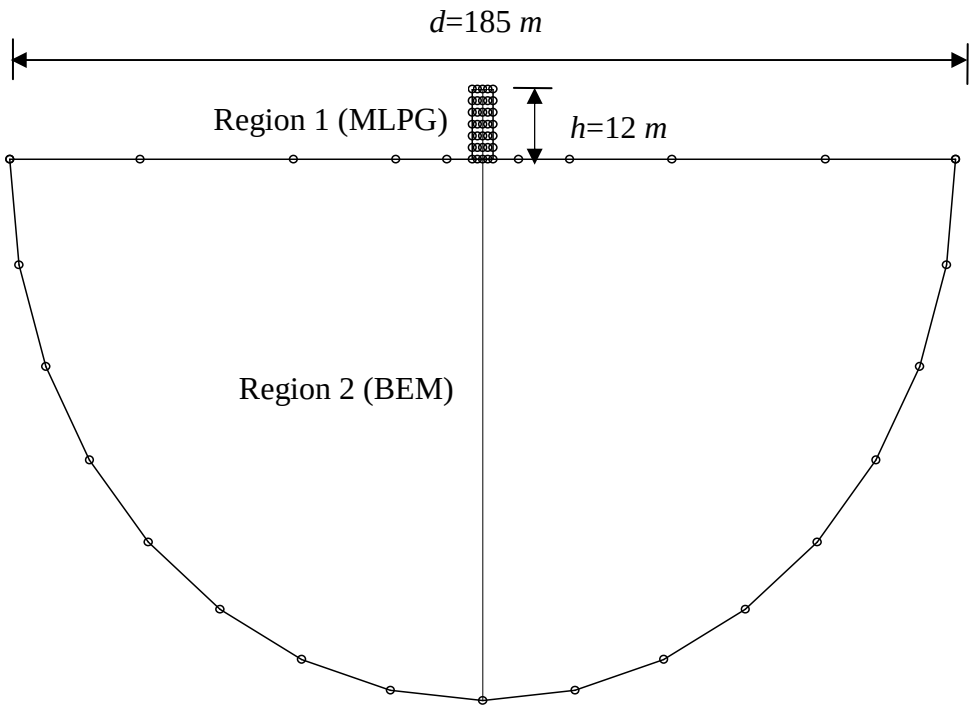


Figure 11 Nodal arrangement of the coupled MLPG/BE method for the problem of a structure standing on a semi-infinite foundation

Liu and Gu : Figure 11

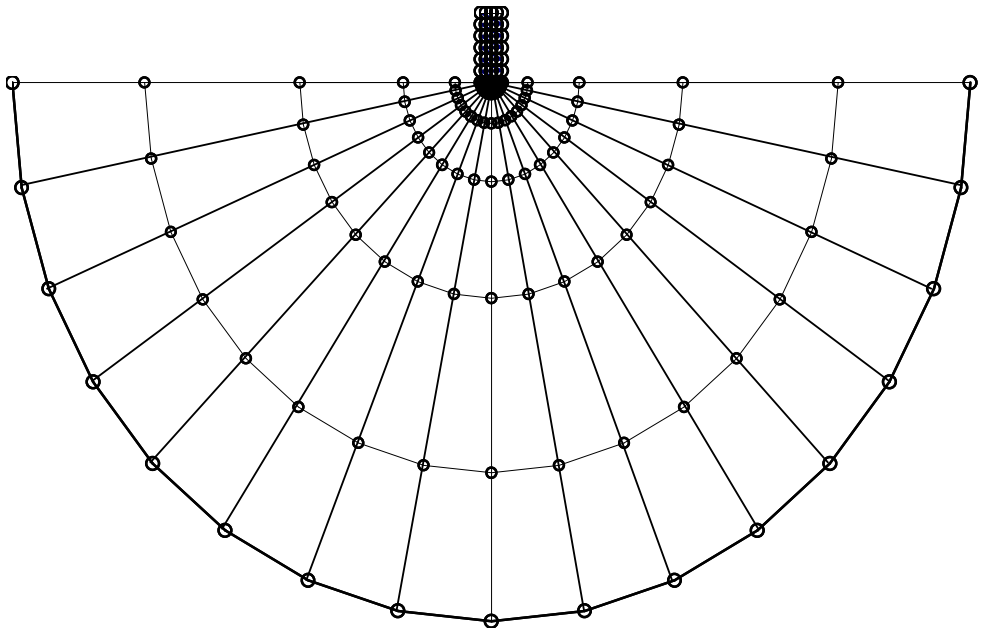

Figure 12  Nodal arrangement of the coupled MLPG/FE method

Liu and Gu : Figure 12

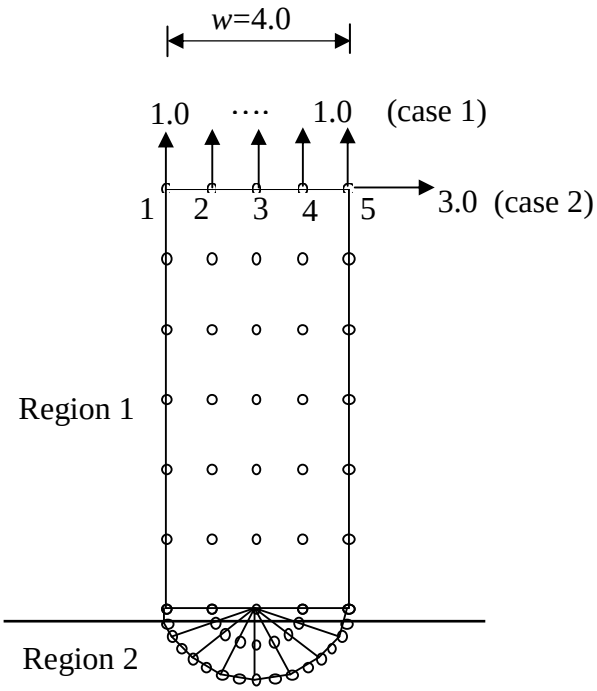


Figure 13 MLPG/FE detailed nodal arrangement of the structure and load cases

Liu and Gu : Figure 13